Gas-phase IR Spectroscopy of Nucleobases.

Mattanjah S. de Vries*

* Department of Chemistry and Biochemistry, University of California, Santa Barbara, California 93106, U.S.A.

Abstract.

IR spectroscopy of nucleobases in the gas phase reflects simultaneous advances in both experimental and computational technique. Important properties, such as excited state dynamics, depend in subtle ways on structure variations, which can be followed by their infrared signatures. Isomer specific spectroscopy is a particularly powerful tool for studying the effects of nucleobase tautomeric form and base pair hydrogen bonding patterns.

Keywords nucleobases, IR spectroscopy, hole burning, REMPI, R2PI, clusters, gas phase

Abbreviations

DRS	double resonant spectroscopy
A	adenine
C	cytosine
G	guanine
T	thymine
U	uracil

1 Introduction

Gas-phase techniques provide a reductionist approach to the study of nucleobases and nucleotides. Collision free conditions *in vacuo* provide insight in the intrinsic properties of individual molecules, free of any interactions. Without such isolation many fundamental properties can be masked by the biological environment, such

as the macromolecular structure of the double helix, base pairing interactions, and the role of the solvent. Among the properties of interest are conformational preferences, tautomeric population distributions, hydrogen bonded and pi-stacking structures, inter- and intra molecular interactions, and excited state dynamics. Once such properties are mapped out for isolated bases, one can hope to extrapolate to more complex systems, including larger DNA segments and solvent contributions. Many aspects of these properties can be probed with the help of IR spectroscopy, which is particularly diagnostic for structural variation, especially when hydrogen bonding is involved.

In order to derive structural information from infrared frequencies, input is required from quantum chemical calculations at computational levels that match the experimental resolution. Experimentally, gas-phase conditions imply extremely low sample densities requiring special techniques in order to acquire infrared data. Some of those techniques involve double resonance approaches that provide unique opportunities for isomer selective IR spectroscopy. This facet is among the advantages of gas-phase experiments making it possible to follow certain properties, such as excited state dynamics, as a function of molecular structure. At the same time the availability of gas phase data provides opportunities to calibrate computational methods, force fields, and functionals.

2 Techniques

Gas-phase spectroscopy of neutral molecules, as opposed to ions, usually involves the use of supersonic molecular beams (1-4). For smaller compounds this can be achieved by seeding in the inert drive gas. This limitation excludes the study of neutral nucleosides or larger compounds while even some of the bare nucleobases, such as guanine, cannot be sufficiently heated without thermal degradation. Some work with bases and base mimics has been done in seeded beams (5-10). Larger compounds can now be vaporized successfully by pulsed laser desorption, followed by entrainment in a supersonic jet (11-14). This experimental advance has opened up the field of study of nucleobases and nucleosides in isolation in the gas phase, especially by IR spectroscopy. The cooling in molecular beams makes this approach particularly attractive for spectroscopy. Although temperatures are not as low as in ion traps or helium droplets, molecular beams can achieve internal temperatures typically of the order of 10 to 20 ^{o}K, which provides very useful optical resolution.

In a supersonic beam typical densities are of the order of 10^{12} molecules/cm^3. Therefore at a typical absorption cross section of 10^{-18} cm^2, a 1 mm supersonic

beam would absorb a fraction of 10^{-7} of incident photons. The low densities inherent in gas-phase experiments have led to the development and application of a number of suitable techniques in order to acquire infrared spectra.

IR-UV double resonance

Most of the work described in this chapter involves action spectroscopy in the form of IR-UV double resonance spectroscopy (DRS). In this approach a secondary step reports on the absorption of the IR photon. A disadvantage is that the resulting spectrum is not a pure absorption spectrum but rather the composite result of two processes. An advantage can be that the secondary step can provide additional information. In the case of IR-UV double resonance one combines direct IR absorption with either resonance enhanced multi-photon spectroscopy (REMPI) or laser induced fluorescence (LIF). A promising new variant is Ionization Loss Stimulated Raman spectroscopy (15). The optical selection of the second step makes these techniques isomer selective, which is their greatest strength. Comparison is sometimes possible with direct absorption techniques, although those generally lack isomer specificity, such as the following:

Fourier transform microwave spectroscopy

In Fourier transform microwave spectroscopy isomeric analysis is derived from rotational spectra, see chapter XXX . Alonso and coworkers have combined this approach with laser desorption jet cooling for the study of tautomeric forms of nucleobases. This technique identified tautomeric forms for all the canonicl bases (16-19), as well as for several of their complexes with water (20), allowing comparisons with tautomer identifications from IR techniques.

Helium droplets

In helium droplets spectroscopy is usually performed in the infrared (21-23). Resonant absorption by specific vibrational modes implies heating, resulting in helium atoms boiling off the droplets, recorded in a mass spectrometer or with a bolometer. This constitutes a direct absorption measurement. The temperature in helium droplets is lower than in supersonic expansions and the cooling is so fast as to essentially freeze the starting population distribution. The starting temperatures need not be elevated much above room temperature because “pick-up” sources do not require very high gas densities.

Cavity ringdown spectroscopy and multi pass absorption

Direct absorption probabilities can be enhanced by multi pass arrangements and a particularly elegant and sensitive form of this principle is cavity ring down spectroscopy, where signal damping is recorded, rather than direct absorption. However, even at the largest ringdown times achievable with the highest quality mirrors, it is still difficult to measure IR absorption in a molecular beam. Saykally and coworkers obtained IR spectra of uracil and of nucleobase clusters with water by

combining cavity ringdown and multi pass spectroscopy with a slit nozzle, that produced an unusually wide molecular beam (24-26).

3 Monomers and tautomeric forms

The nucleobase monomers can adopt a variety of tautomeric forms and IR spectroscopy in the near IR is diagnostic for this property, especially with the NH and OH stretch frequencies as fingerprints of keto, imino, or enol forms.

3.1 purines

Figure 1 shows IR frequencies for guanine as calculated by Marian (27). The enol forms are characterized by the OH stretch at about 3600 cm^{-1}, marked in red, and a red shift of the symmetric and antisymmetric NH_2 stretches, marked in blue and purple, respectively. The imino forms are characterized by the imino NH stretch below 3400 cm^{-1}, marked in orange, which is however very low in intensity and therefore not diagnostic in most experimental spectra. The N1H and N3H stretches are marked in dark and light green, respectively. Pairs of tautomers that only differ in the N7H versus N9H form, such as (a) *vs* (b) or (c) *vs.* (e), have very similar IR signatures. The N7-H and N9-H frequencies are almost identical at about 3500 cm^{-1}, marked in grey. Sometimes tautomeric blocking by methyl substitution or deuteration can help resolve assignments [mons]. An analogous problem, which can not be resolved by substitution, is the similarity in IR signature of conformational tautomers, such as (g) *vs.* (h) or (c) *vs.* (d). Because of this complication, assignments with complete confidence call for computational data at very high resolution. This requirement is problematic, especially since currently available computations do not account for anharmonicity and thus employ scaling factors that are not rigoursly defined.

Four species have been observed in REMPI spectra, labeled A-D, distinguished by UV-UV hole burning and characterized by IR-UV DRS. Panels (c) and (g) in Figure 1 show experimental spectra from Nir et al., obtained by IR-UV DRS. Originally these tautomers were assigned as the four lowest energy forms, with A and D as enol forms and B and C as keto form. The N7 *vs.* N9 forms of each were subsequently distinguished by mons et al. by selective methyl substitution (28). However, the B,C assignment to the keto form turned out to be incorrect. Surprisingly, these are imino forms, even though these tautomers are significantly higher in energy, and the three lowest energy tautomers are thus absent in the REMPI spectra (27,29). This absence is explained by short, sub-picosecond, excited state lifetimes, to be discussed below, which render nanosecond timescale REMPI blind

for these tautomers. The three “missing” tautomeric forms are shown in red in Figure 1. Evidence that these tautomers are in fact present in the gas phase comes from two other experiments that are direct absorption measurements, as opposed to action spectroscopy, and thus do not involve the excited state. One is FT microwave spectroscopy by Alonso et al., who observe the 4 lowest energy tautomeric forms (a)→(d) (18). The second evidence comes from a helium droplet experiment by Choi and Miller who found the same four lowest energy tautomers (30). These experiments are not isomer selective so a large number of vibrational bands are observed in the infrared spectrum. The assignment was aided by aligning the molecules in an electric field and recording absorption as a function of the polarization angle of the light relative to the field. This elegant approach provides vibrational transition moment angles as additional data for comparison with ab initio theory.

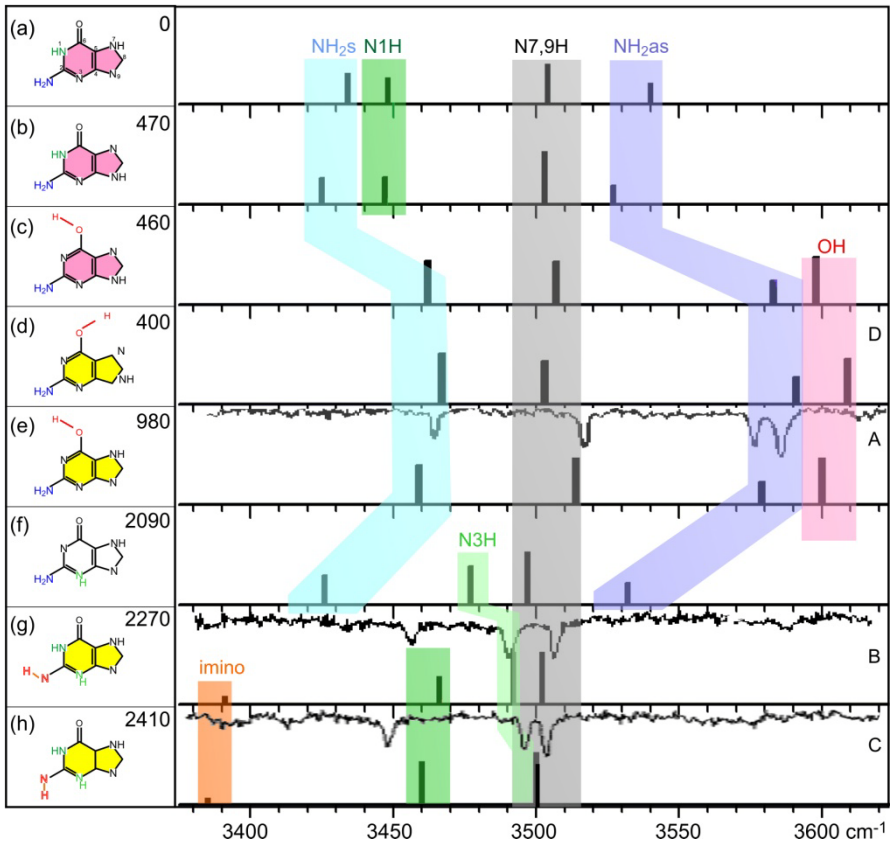

Figure 1. IR frequencies for the 8 lowest energy guanine tautomers, as calculated by Marian (27). Modes are color-coded as shown in the structures on the left. Color coding of the structures is detailed in the text. Numbers are relative energies in cm^{-1}. Panels (e), (g) and (h) show experimental IR-UV double resonance spectra from Nir et al (31). The labels A-D refer to the four tautomers observed in REMPI spectroscopy.

Seefeld et al. confirmed the assignment of the B and C tautomers to the imino form by measuring the imino C=N stretch frequency at ~1700 cm^{-1} (32). Figure 1 shows the resulting final assignments of the four long-lived tautomers A-D in yellow.

Nir et al. obtained IR-UV DRS spectra of a series of guanosines, some of which appear in Figure 2 (31). Trace (a) shows 9H enol guanine (trace (c) in Figure 2) for comparison. The peak at 3525 cm^{-1} marked in yellow corresponds to the 9H stretch and is absent in all the guanosine traces: (b) 2',3'-deoxyguanosine, (c) 3'-deoxyguanosine (d) 2'- deoxyguanosine,, and (e) guanosine. The blue and purple bands denote the symmetric and antisymmetric NH_2 stretch modes, while the red band denotes the OH stretch, showing that all these guanosines are in the enol form. As is the case with bare nucleobase, the keto form is not observed wih anosecond timescale REMPI. The red peaks correlate with the 2'-OH and the blue peaks correlate with the 3'-OH modes. The small red shift of the 3'-OH mode in trace (e) compared to trace (d) indicates a small amount of hydrogen bonding, consistent with a "windshield wiper" orientation with the 3'-OH pointing towards the 2'O. The 5'-OH frequency is absent in this frequency range, presumably due to strong red shifting, suggesting a strong internal hydrogen bond consistent with a *cis* orientation of the sugar.

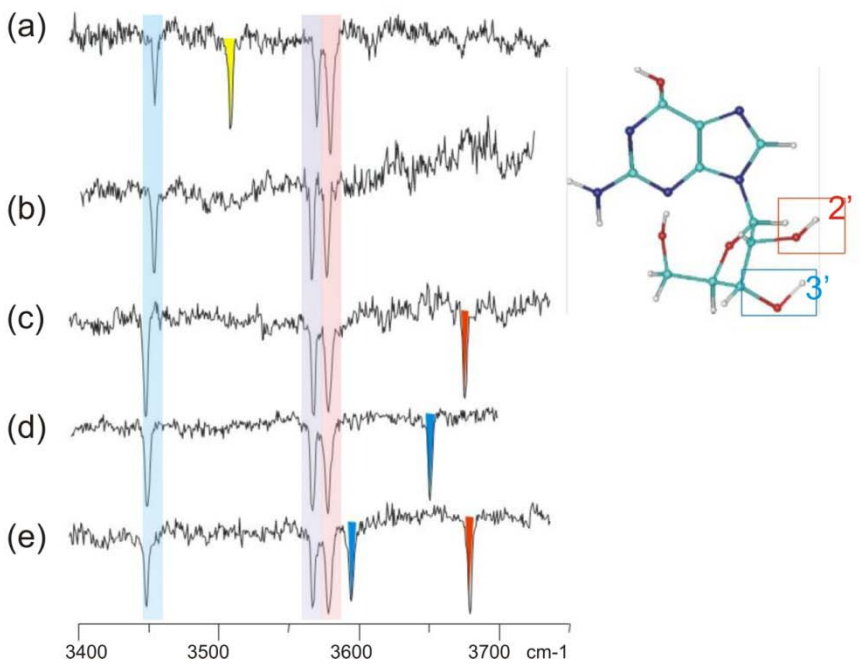

Figure 2: IR-UV DRS spectra of (a) guanine, (b) 2',3'-deoxyguanosine, (c) 3'-deoxyguanosine (d) 2'- deoxyguanosine,, and (e) guanosine.

The near IR range between 3000 and 4000 cm^{-1} is very diagnostic for structure since it contains the N-H and O-H stretches. Inclusion of the C=O stretch frequency around 1800 cm^{-1}, which now becomes possible with table-top laser systems, extends the useful range further. The mid IR range, typically 500-2000 cm^{-1}, attainable with a free electron laser, usually does not add much extra structural information. Those lower frequency modes can add further detail, however, especially for the sugar in nucleosides. Figure 3 shows IR-UV DRS spectra obtained at the FELIX free electron laser facility of (a) guanosine and (b) 2'-deoxyguanosine. The red peaks correspond to modes in the guanine, while blue colored peaks denote modes of the sugar moiety. Trace (c) shows the spectrum of 9-ethyl-guanine for comparison, with the main ethyl modes marked in yellow.

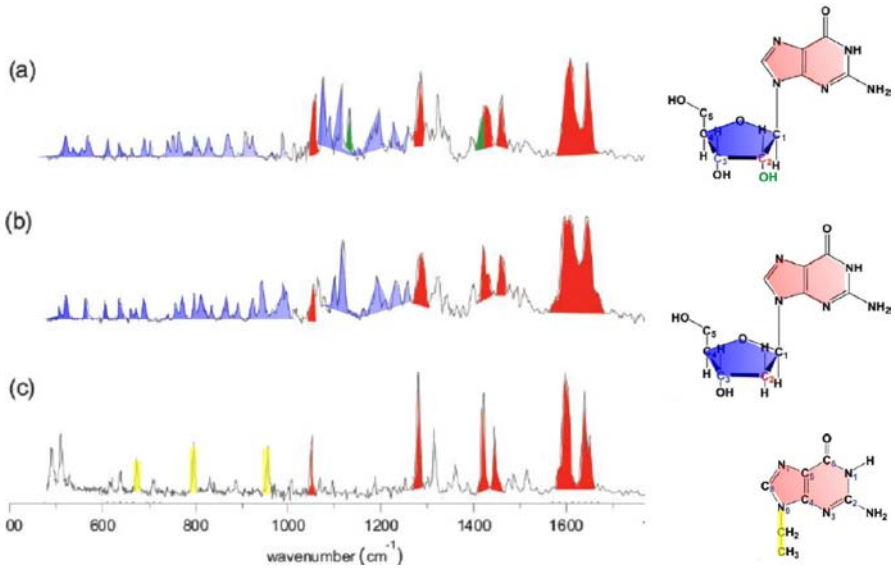

Figure 3: IR-UV DRS spectra of (a) guanosine, (b) 2'-deoxyguanosine, and (c) 9-ethyl-guanine.

The tautomeric landscape of adenine is somewhat less varied than in the case of guanine because of the absence of the oxygen. Plützer and Kleinermanns reported IR-UV double resonance and observed two tautomers, for which Figure 4 shows the IR spectra (5,33). Both tautomers are of the amino form, with the 9H form by far the most abundant relative to the 7H form. This finding is consistent with the microwave measurements by Brown et al. (34). At the conditions of jet cooling, the imino form appears to be absent, although in the gas phase at elevated temperature the IR spectra seem to comprise multiple tautomers, including imino. The analysis is somewhat complicated by the fact that the UV spectra contain contributions to two excited states, of $\pi\pi^*$ and $n\pi^*$ character respectively (35,36).

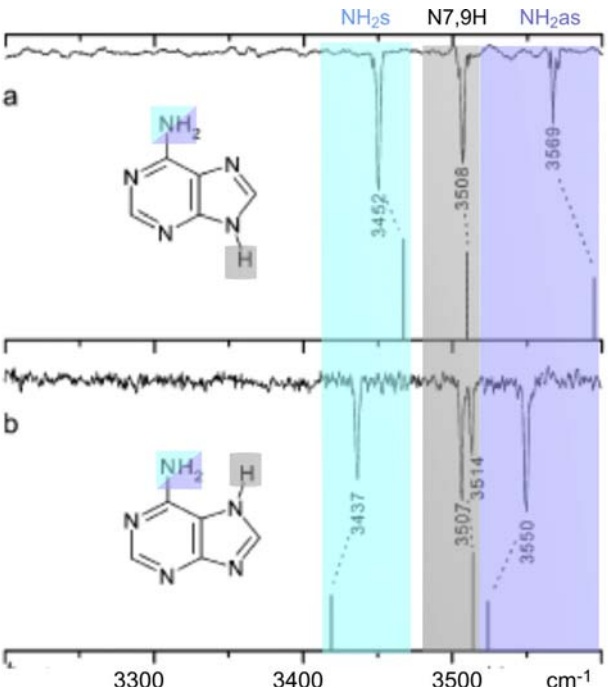

Figure 4: IR-UV double resonance spectrum of adenine with the R2PI laser tuned to (a) 36 105 cm-1 and (b) 35 824 cm-1. The stick spectrum shows the vibrational frequencies calculated at the B3LYP/6-311G(d,p) level. Data from Plützer and Kleinermanns (reprinted with permission, color coding added) (33). Stick spectra were computed at the B3LYP/6-31G(d) level with a scaling factor of 0.9613.

3.2 pyrimidines

Figure 5 displays the main tautomers observed for the pyrimidine bases. Cytosine appears in both the keto and enol form, while uracil and thymine each appear almost exclusively in the diketo form. The IR-UV DRS spectrum of keto-cytosine appears in trace (a) of Figure 6, with 1-methyl and 5-methyl derivatives for comparison in traces (b) and (c) respectively. The two enol forms for cytosine cannot be distinguished realistically by available IR spectra. The enol tautomer is slightly more stable than the keto form by about 0.03 eV (37-39). The keto form is the biologically important one, with Wtason-Crick base pairing in DNA, and predominant in solution. The keto-imino form in cytosine is much higher in energy. In matrix isolation Szczesniak et al. observed both keto and enol forms with higher abundances for the latter and small contributions from the imino form (40). Brown et al. have obtained rotational constants for all three tautomeric forms by microwave spectroscopy (41).

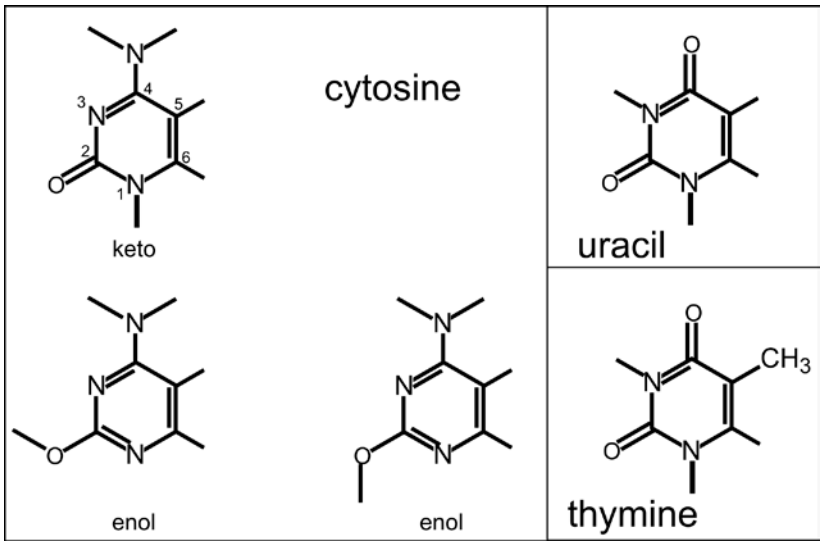

Figure 5: structures of lowest energy tautomers of the canonical pyrimidine bases.

While the energy difference between the enol and keto forms is very small, some of their other properties, such as their vertical excitation energies, are very different. Nir et al. reported REMPI and hole burning spectra and concluded that the keto and enol tautomers have band origins that differ by a remarkable half electron volt at 314 nm and 278 nm, respectively (42,43). The REMPI spectra of U and T exhibit a very broad structure with an onset in the frequency range of the origin of the enol cytosine first reported by Brady et al. (4).. No spectroscopic detail could be extracted from these broad spectra and tautomeric information was limited for a long time to bulk measurements.

Microwave measurements of uracil in a heated cell suggested the diketo form as the most abundant (44). Brown et al. reported the first microwave measurements in a seeded molecular beam and also concluded that the diketo form was predominant (45). Viant et al. reported the first rotationally resolved gas phase IR spectra of uracil (26). This work employed a slit nozzle, an IR diode laser, and a multipass arrangement to obtain high resolution IR absorption spectra of the the out-of-phase $\nu_6(C_2{=}O, C_4{=}O)$ stretching vibration. The rotational analysis unambiguously assigned the species to the diketo tautomer. Brown et al. also observed the diketo form of thymine in a seeded molecular beam, based on the hyperfine structure in the $14_{4,10}$-$13_{3,11}$ transition (46).

Recently Ligare et al. confirmed the diketo character of the broad absorption of both U and T by IR-UV DRS. Their spectra showed ion gain rather than dips upon IR excitation. Double resonant spectroscopy relies on the fact that the burn laser changes the ground state vibrational distribution and thus the overall Franck-Condon (FC) factors. When the probe laser is tuned to a strong resonance, this invariably leads to ion dip. However, in the case of a broad absorption, the consequences of modified FC factors are not always predictable and an ion dip may not necessarily occur. In the case of U and T it is likely that there is a large geometry change between the ground state and the excited electronic state, which leads to more favorable FC factors and thus ion gain. Such a scenario would also help explain the gradual onset of the REMPI spectrum and the absence of a strong 0-0 transition.

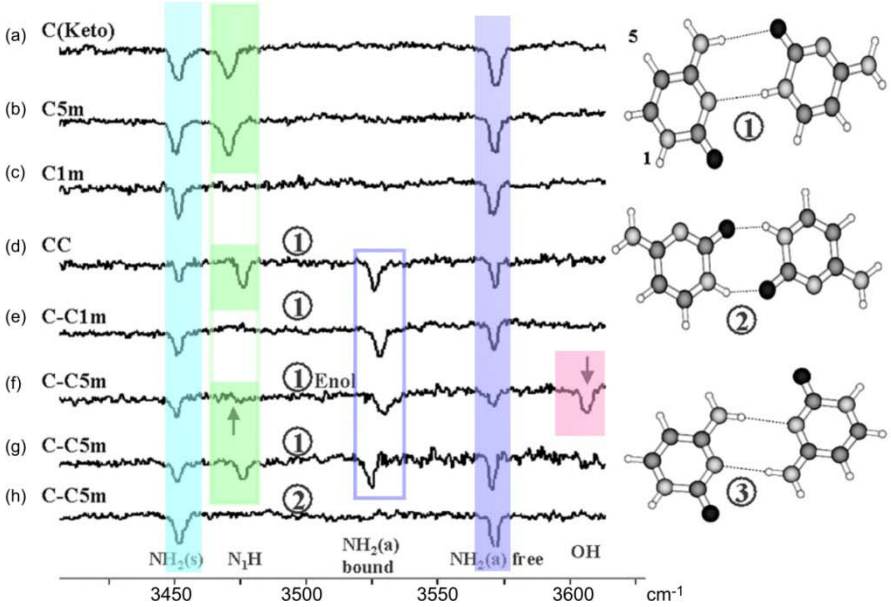

Figure 6: IR-UV DRS spectra of cytosine monomers (a-c) and dimers (d-h). C1m and C5m denote 1-methylcytosine and 5-methylcytosine, respectively. Circled numbers on the dimer traces refer to the cluster structures shown on the right. Traces f-h were recorded at three different UV wavelengths, corresponding to three different structures of the C-C5m cluster.

3.3 Excited state IR

An additional reason for excited state broadening may be lifetime broadening. As will be discussed below, most of the $\pi\pi^*$ excited state returns to the ground state on a picosecond time scale by internal conversion. However, there is a small quan-

tum yield for a process leading to a "dark" excited state of nπ* character or a triplet state ($^3\pi\pi^*$ or $^3n\pi^*$). Kunitski et al. have characterized this dark state for 1-methylthymine by performing IR-UV DRS on the excited stat, rather than the ground state (47). Figure 7 shows the spectra obtained for the NH stretch. The bottom trace is the usual ground state IR-UV DRS spectrum. The help trace results from eight different pulse sequence in which the molecule is first excited by the pump laser and partly relaxes into the dark state, which is subsequently subjected to be IR burn pulse and ionized by the probe pulse. The result is a small red-shift, interpreted as characteristic for a triplet state, whereas an nπ* state would have produced a blue shift. Ligare et al. have recently obtained similar results for thymine itself.

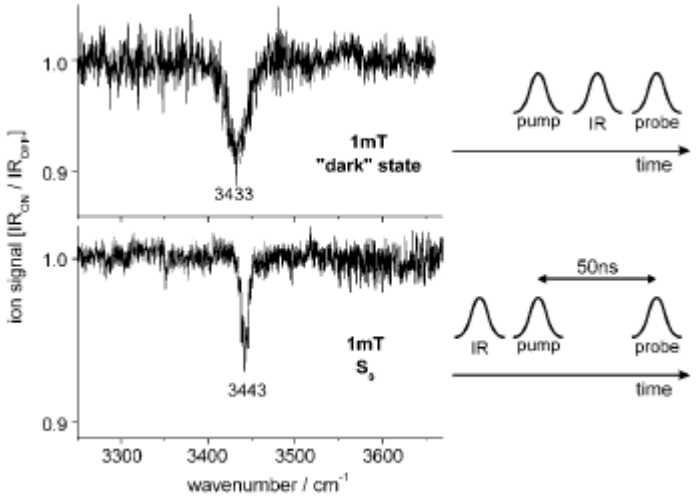

Figure 7: Ionization-detected IR spectra of 1-methylthymine in the ground state (bottom) and long lived transient excited state (top) in the NH/OH stretch region. The corresponding laser pulse sequences are shown on the right (47).

3.4 ionic nucleobases and nucleotides

For nucleotides the charge on the phosphate group generally precludes the use of the IR-REMPI hole burning technique. Instead it is possible to study ions in a trap by IR multiphoton dissociation (IRMPD). The characteristics of a free electron laser, such as FELIX, with its macro and micro pulses, are very suitable for this type of multiphoton IR spectroscopy. Since there is no isomer selection in this case, the interplay with theory is especially important and the occurrence of multiple structural forms could complicate interpretation. van Zundert et al. compared results

for neutral (by DRS) and protonated (by IRMPD) adenine and 9-methyladenine in the same mid IR frequency range of 525-1750 cm^{-1} (48). They found the 9H tautomer to be dominant for both neutrals and ions. Salpin et al. studied protonated uracil, thymine, and cytosine by IRMPD spectroscopy (49). Calculated infrared frequencies of the different low-lying isomers (computed at the B3LYP/6-31++GACHTUNGTRENUNG(d,p) level) predict the global energy minimum for an enolic tautomer in each case, whose infrared absorption spectra matched very well with the experimental IRMPD spectra. An additional very weak IRMPD signal observed at about 1800 cm^{-1} suggests the presence of the second lowest energy oxo tautomer. Oomens et al. studied protonated cytosine dimers, concluding that the proton moves from one basic atom to another when the dimer ion dissociates (50). Yang et al. studied the effect of C5 substituents on the cytosine base pairing motifs and conclude that the substitution does not alter the lowest energy base pairing structures (51,52). Yang et al. found a single tautomer for alkali metal cation cytosine complexes (53), as did Nei et al. for sodiated uracil and thiouracil complexes (54,55). On the other hand, Crampton et al. found that protonation preferentially stabilizes minor tautomers of halouracils (56).

Nei et al. have reported the IR spectra of all deprotonated canonical nucleotides, trapped in a FTICR instrument and subjected to IRMPD in the mid-IR (57,58). The measured IRMPD action spectra were compared to the linear IR spectra calculated at the B3LYP/6-311+G(d,p) level of theory and the most stable conformations of the deprotonated forms of dA5'p, dC5'p, and T5'p were found to be conformers where the ribose moiety adopts a C3' *endo* conformation and the nucleobase is in an *anti* conformation. By contrast, the most stable conformations of the deprotonated form of dG5'p are conformers where the ribose adapts a C3' *endo* conformation and the nucleobase is in a *syn* conformation. In addition to the ground-state conformers, several stable low-energy excited conformers that differ slightly in the orientation of the phosphate ester moiety were also accessed in the experiments. Comparison of the conformations found by these authors for DNA nucleotides *vs* RNA nucleotides would suggest that the intrinsic difference between the DNA and RNA mononucleotides is most likely not due to their relative conformations but due to the change in their chemical properties induced by the different substituents at the C2′ position(57). By the same technique Ligare et al. studied deprotonated clusters of nucleotides and found that unlike in multimer double stranded DNA structures, the hydrogen bonds in these isolated nucleotide pairs are predominantly formed between the phosphate groups, as shown in Figure 8.

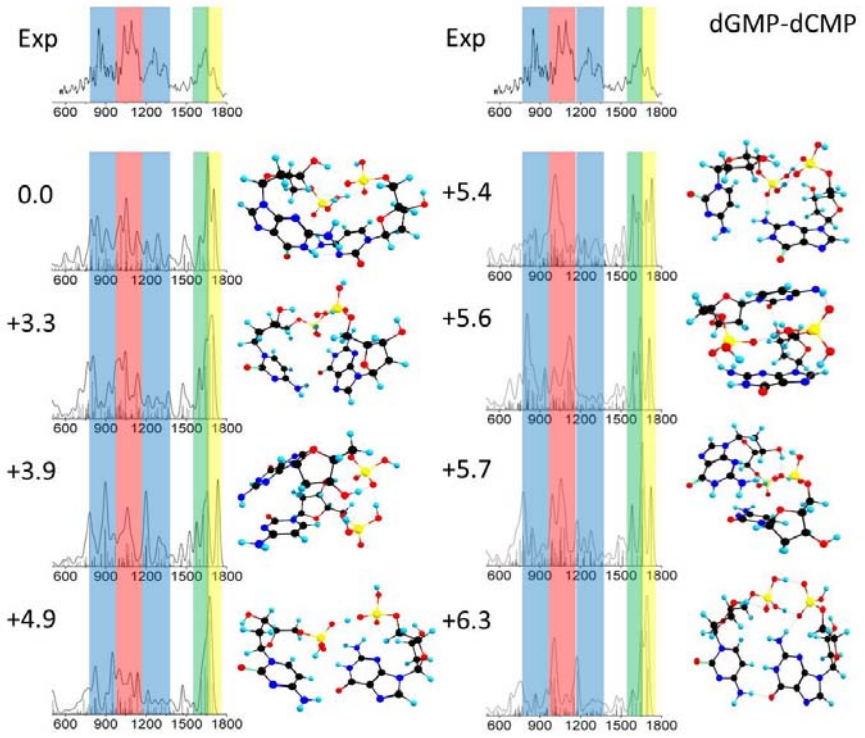

Figure 8: The six lowest calculated energy spectra for deprotonated [dGMP-dCMP]- compared with IRMPD experiment. The energies listed are Gibbs free energies in kcal/mol relative to the ground state structure (59).

4 Cluster structures

IR spectroscopy is also very diagnostic for the structure of hydrogen bonded clusters. Upon hydrogen bonding, NH and OH stretch frequencies in the near IR generally shift to the red by often hundreds of wavenumbers while also broadening. The extent of the red-shift is correlated with the strength of the hydrogen bond. The red-shift and broadening cannot be computationally predicted with much accuracy, however they are very clear indicators showing which hydrogen bonding sites are implicated in bonds, while frequencies that do not shift mark the free sites. Therefore near IR spectra can provide insight in the cluster structure, often to the point of complete structural assignment.

4.1 base pairs

Figure 6 demonstrates this principle for cytosine dimers: Traces (c)-(g), with both a free and a bound (shifted) NH_2 vibration clearly point to structure 1. Trace (h) with only free NH_2 is consistent with structure 2, while structure (3) can be excluded for all of these spectra since it would contain no free NH_2 modes. Furthermore the 3600 cm^{-1} OH frequency, characteristic for the enol form, appears only in trace (f).

Figure 12 shows IR-UV spectra for three structural isomers of GC base pairs (60). The stick spectra are DFT calculated vibrational frequencies for the structures shown in the insets. Structure A is the Watson-Crick structure, while structure C is almost the same structure, however the cytosine is in the enol form instead of in the keto form. This subtle tautomeric difference has a dramatic effect on the photophysical properties as will be discussed below. The IR-UV spectrum in trace (a) correlates with a broad, structureless UV spectrum. The fact that broad UV absorption yields a sharp IR-UV hole burning spectrum is somewhat fortuitous. The IR burn pulse excites a specific vibrational mode around 3000 cm^{-1}, followed by internal vibrational redistribution (IVR) on the picosecond time scale. The resulting vibrational state populations produce a different Franck Condon landscape, which for a broad absorption may or may not lead to depletion of the UV probe signal. In fact, it is possible that the new FC landscape leads to a gain in ionization signal, as observed for uracil and thymine. Mayorkas et al. also observed gain signals in ionization loss stimulated Raman spectroscopy of tryptamine conformers (61). Similarly, gain signals are possible following excitation in the mid IR which imparts a small amount of energy and thus provide less opportunity of vibrational redistribution.

A particular computational challenge is the incorporation of anharmonicity of the potentials. A common fix is the application of scaling factors but this approach, while useful, is clearly fraught with uncertainty. While it is good practice to always use the same empirical factor for consistency, it is also reasonable to assume that different modes could require different factors, leaving one with a somewhat uncomfortable number of empirically adjustable parameters. In the quest to develop more comprehensive computational strategies it is useful to be able to compare with both near- and mid-IR data as sensitive tests. Figure 9 shows such a comparison for the GC base pair with the cytosine in the enol form, as depicted in trace (c) in Figure 12 (62). The mid IR part of this spectrum (left panel) was obtained at FELIX and the lower frequencies provide an especially sensitive test for theory. Comparison of the theoretical frequencies with the experimental results indicates that the average absolute percentage deviation for the methods is 2.6% for harmonic RI-MP2/cc-pVDZ (3.0% with the inclusion of a 0.956 scaling factor that

compensates for anharmonicity), 2.5% for harmonic RI-MP2/TZVPP (2.9% with a 0.956 anharmonicity factor included), and 2.3% for adapted PM3 CC-VSCF; the empirical scaling factor for the ab initio harmonic calculations improves the stretching frequencies but decreases the accuracy of the other mode frequencies.

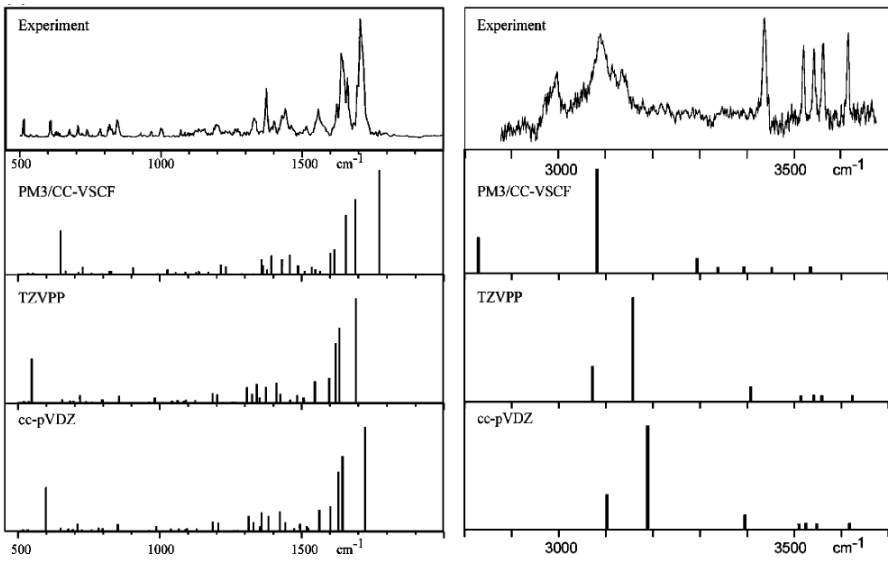

Figure 9: Comparison of experimental data with calculations according to different models aimed at correcting for anharmonicity (62).

This work is an example of the ongoing cross fertilization of theory and experiment, in which gas-phase data serve as benchmarks for computational method development, while the computations provide the analysis of the experimental results.

For AT base pairs Plützer et al. reported the IR-UV spectrum, which they assigned to cluster structures with (HNHO)-O-...=C/(NHN)-H-... hydrogen bonding by comparison with ab initio calculated vibrational spectra of the most stable A-T isomers [63]. The Watson-Crick A-T base pair is not the most stable base-pair structure at different levels of ab initio theory, and its vibrational spectrum is not in agreement with the observed experimental spectrum. This is directly shown by the free N3H vibration in the IR spectrum of AT. This group is involved in hydrogen bonding in the Watson-Crick pair. Experiments with methylated A and T further support the structure assignment.

4.2 Clusters with water

IR-UV DRS also lends itself to analysis of clusters with water in order to study the details of hydration, one water molecule at a time. Figure 10 shows IR-UV spectra of guanine water clusters as an example (64). Traces (a)-(c) show spectra from three observed structures while panels (d)-(f) show spectra from corresponding non-hydrated structures for comparison. The hydrated spectra contain broad, red-shifted peaks due to hydrogen bonded modes, but the free modes suffice for analysis. They each contain a free water OH stretch, excluding bridged structures. Traces (a) and (b) parallel trace (d). Panel (b) contains the free enol OH mode. Panel (a) is almost identical but without the enol OH mode indicating an enol with the water bound to the OH. Trace (c) parallels traces (e) and (f), missing both NH_2 modes as well as the enol mode but showing the N3H and N1H mode characteristic for the imino form. Once again, the keto form is not observed in these experiments. Chin et al. also reach that conclusion in their detailed study of rotamers of 9-methylguanine with water (65,66).

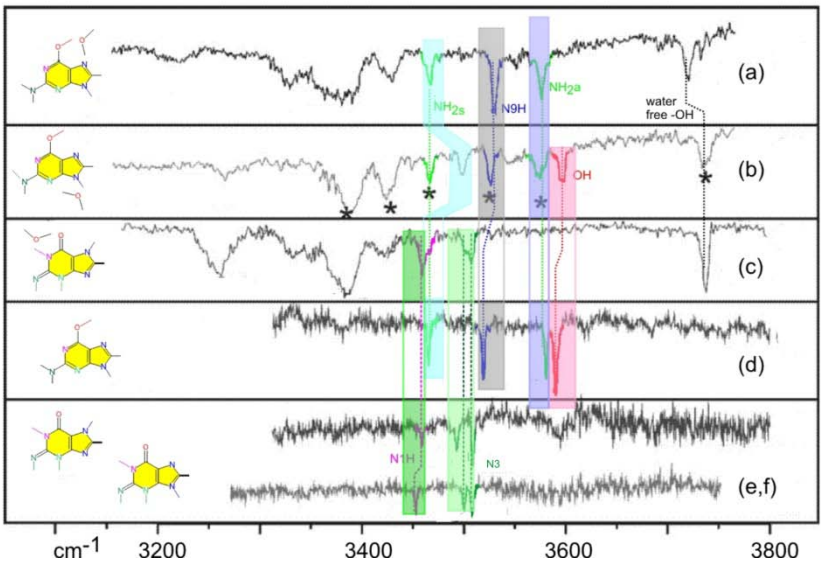

Figure 10: IR-UV hole burning spectra of guanine with (a-c) and without (d-f) water. Corresponding modes for corresponding structures with and without water are indicated by dotted lines and color coding. Structures are schematic only. Asterisks denote peaks in (b) that also show up in (a), probably due to overlap in the probe spectra. Adapted from reference (64).

Saigusa et al. reported IR-UV DRS spectra of hydrated clusters of nucleosides [67,68] and of GG and GC base pairs [69]. For the monohydrated cluster of Gs they found multiple structural isomers. For one of the monohydrates they assigned a hydration structure involving the 5′-OH group of the sugar and the amino group of the guanine moiety. From the IR spectrum of the dehydrated clusters they inferred

that the 2′-OH group is significantly influenced by the addition of the second water, which suggests the possibility of specific dihydrate structures for Gs. Their results also suggest that the amino-keto forms of Gs and 9MG, which are missing in the REMPI spectrum, can be observed upon hydration.

4.3 Stacking *vs.* H-bonding structures

Two structural motifs dominate in DNA: π-stacking provides most of the structural stability of the helix while hydrogen bonding provides most of the recognition properties. For pairs of single bases H-bonding is the exclusive motif in the gas phase while stacking dominates in solution. Water molecules stabilize the stacked structure both by competing with hydrogen bonding sites on the bases and by stabilizing the structure by forming bridges. Hobza and coworkers have calculated how many water molecules are needed to lead to preferential stacking and concluded that depending on the base pair this number can range from two to five (70,71). Clusters of that size have not yet been characterized in the gas-phase so this transition has not yet been experimentally verified. Another way to encourage stacking is blocking hydrogen bonding sites by methylation and several examples have been reported.

Callahan et al. have used xanthine and its methylated derivatives as models for studying the two motifs (72,73). For the 7-methylxanthine dimer, they observed hydrogen bonding on the N3H position suggesting 3 possible combinations, one that is reverse Watson–Crick type and two that are reverse Hoogsteen type. For the 3-7-dimethylxanthine dimer, they observed a stacked structure, as determined by the free N1H stretch frequency. For trimethylxanthine dimers they inferred a stacked structure as well.

Plützer et al. reported a stacked structure for 9-methyladenine-adenine (9mA-A) clusters based on one free NH_2 group and one weakly interacting NH_2 and N9H group in the IR-UV spectrum (74). They found no evidence of stacking for A-A, 7mA-A, or 9mA-9mA clusters. The latter shows only broad vibronic structure and is probably symmetrically hydrogen bound via the NH_2 groups. Interestingly, the symmetrically bound A-A cluster structure was not observed, although it is predicted to be the lowest in energy. Smith et al. studied adenine and microhydrated $A_m(H_2O)_n$ clusters by femtosecond pump–probe mass and photoelectron spectroscopy (75). For the predominantly hydrogen-bonded adenine dimer, excited state relaxation is dominated by monomer-like processes. But when the adenine dimer is clustered with several water molecules, they observed a nanosecond lifetime ascribed to excimer states in π-stacked clusters.

Asami et al. reported IR-UV DRS spectra for base pairs of adenine nucleosides, adenosine (Ado) and N6,N6-dimethyladenosine (DMAdo) (67). They found that

the dimer possesses a stacked structure, stabilized by the formation of a hydrogen-bonding network involving the two sugar groups. The occurrence of the frequency shift and broadening is explained satisfactorily based on the anharmonic coupling of the OH stretching modes with specific bending modes and low-frequency modes of base and sugar moieties. By contrast, Saiguse et al. performed experiments with GG and GC pairs with methyl substitutions in the sugar position, which for GC forces the Watson-Crick structure. The IR markers for this structure remained essentially unchanged upon hydration, suggesting no significant structural change nor stabilization of π stacking (69).

5. Excited state dynamics.

With the ability to perform isomer selective IR spectroscopy has come the opportunity to study effects of subtle structural variations. One of the remarkable outcomes is that certain low energy isomers have not been observed in IR-UV DRS. Notable examples are the keto tautomer of guanine and the Watson-Crick structure of the GC base pair. Similarly, the lowest energy symmetrically hydrogen bonded structures of homodimers, such as GG and AA are missing in these IR-UV measurements. Intriguingly these “missing” isomers tend to be the biologically most relevant forms. Inevitably, double resonant spectroscopy involves a form of action spectroscopy, usually two-photon ionization and sometimes laser induced fluorescence. Both techniques detect the excited state. In a number of cases where direct absorption measurements are available the “missing” isomers are in fact observed, implying that they do exist in the gas phase. A prime example is the keto tautomer of guanine, which is identified both in microwave spectroscopy in a molecular beam (18) and in helium droplets (30).

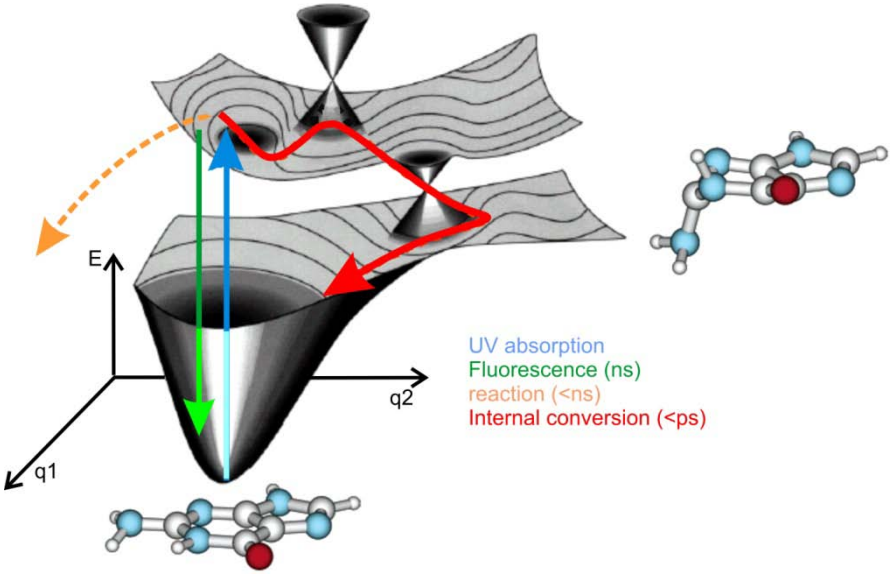

Figure 11: Schematic potential energy diagram as a function of two generic internuclear coordinates, q1 and q2 showing the concept of conical intersections connecting different electronic states. Insets show the geometry of guanine at the ground state equilibrium and at the conical intersection between the ππ* and the SO state, as calculated by Marian (27).

The failure to observe certain isomers can be attributed to short lived electronically excited states. An excited state lifetime of the order of picoseconds or less is in fact four or more orders of magnitude shorter than the typical laser pulses of several nanoseconds, routinely used for two-photon ionization. This fact renders this form of action spectroscopy blind for the species with the shortest excited state lifetimes. A picture is now emerging in which the electronic excited state can undergo rapid internal conversion to the ground state. The key is the occurrence of conical intersections (CIs) that connect the excited state potential energy surface, reached by photon absorption, to the ground state potential energy surface. The dramatic lifetime differences between isomers and derivatives of nucleobases appear to be due to variations in the excited state potential surfaces that restrict or slow access to these conical intersections (76). As illustrated schematically in Figure 11, conical intersections are the crossings of multidimensional potential surfaces. Therefore these features can only occur in regions of the potential energy landscape that represent a deformation of the molecular frame from the ground state equilibrium geom-

etry. For example, Figure 11 shows the geometry at the conical intersection for the keto tautomer of guanine, calculated by Marian (27). The CI involves strong out of plane bending of the C2 coordinates and different tautomeric arrangements lead to different potential surfaces along those coordinates. As a result, other tautomers do not lead to the same trajectories on the excited state potential surface and only the keto form exhibits the barrierless pathway through the CI, producing its sub-picosecond internal conversion. This mechanism also explains the strong dependence of excited state lifetimes on derivative structure (77-79). When a subpicosecond internal conversion pathway is available (indicated schematically in red in Figure 11), it can compete favorably with other processes, such as fluorescence (green) or other photochemical processes (orange).

In the case of the pyrimidine bases, the major coordinates forming the CI are torsion and stretching of the C5=C6 bond. For 4-aminopyrimidine, surface hopping calculations identified two conical intersections (5,33,80-92): deformation at the C2 position leads to deactivation of the excited state with a lifetime, τ^*, of 1 ps and deformation at the C5=C6 bond with a τ^* of 400 fs. Immobilizing the latter with a 5 membered ring forms adenine with a conical intersection due to the C2 deformation, τ^* of 1 ps and dynamics similar to that in guanine. C2 substitution changes the potential energy landscape along this coordinate, such that adenine's isomer 2-aminopurine has a nanosecond excited state lifetime and strongly fluoresces. Similarly, for the pyrimidine bases the oxygen substitution at the C2 position eliminates the CI associated with the C2 puckering but leaves the CI associated with the C5=C6 coordinates available for internal conversion. C5 substituents in pyrimidines further alter excited state lifetimes over a range of picoseconds to nanoseconds, by modification of the topography of the potential energy surfaces around C5=C6 torsion and stretching coordinates(79,93,94). Interestingly, the same coordinates are found to play a role in thymine photo-dimerization in DNA (95).

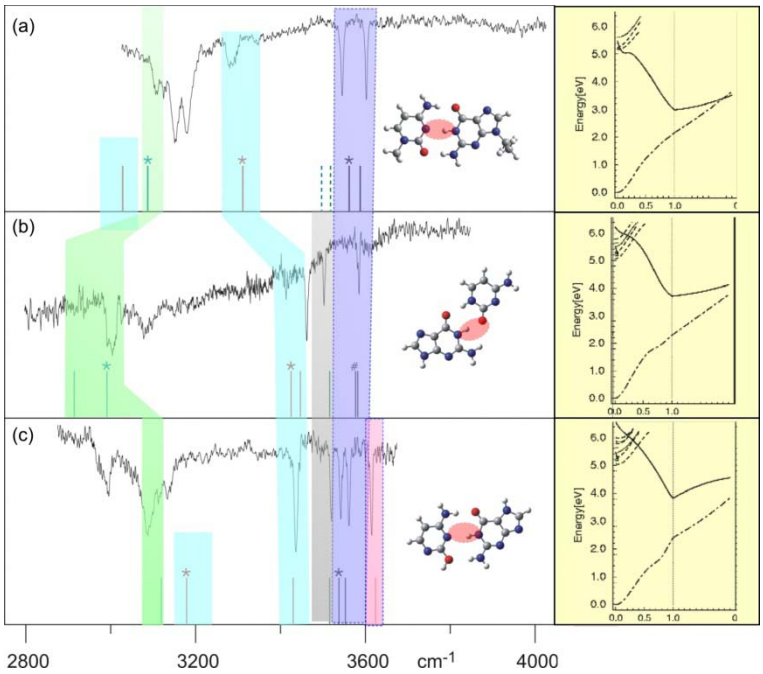

Figure 12: Left column shows three structures (left column) observed for isolated GC base pairs, as identified by IR-UV spectroscopy. Stick spectra are DFT calculated vibrational frequencies. Structure A is the Watson-Crick structure. Right column shows calculated potential curves (ref (96)). A charge transfer state (CT in red) connects the S1 (green) and S0 state (blue) by two conical intersections in A but not in B and C. The reaction coordinate is middle hydrogen motion, N1-H, indicated with a red ellipse in the structures. Color coding of the modes is the same as in Figure Y.

We can now rationalize why for GC clusters the one structure that is prevalent in DNA, the Watson-Crick structure, has not yet been observed by two-photon ionization with nanosecond laser pulses. In the work of Nir et al. only a substituted version (9-ethylG-1-methyl-C) was reported (panel (a) Figure 12 and its corresponding two-photon UV spectrum was very broad. Presumably, the Watson-Crick structure has a sub-picosecond excited state lifetime, while other structural arrangements of the same base pair have sharp spectra, consistent with much longer excited state lifetimes (97). To explain the effect, the right column of Figure 12 shows calculated potential curves from Sobolewski and Domcke (96). The reaction coordinate is hydrogen motion, N1-H, indicated with a red circle in the structures. A charge transfer state connects the S1 and S0 state by two conical intersections in A but not in B and C. The difference in tautomeric form between the A and the C case induces a subtle change in the excited state potential energy

landscape. The charge transfer state is just slightly higher in energy relative to S0 and S1, creating a barrier for reaching the first conical intersection. Thus a small change in potential energies upon tautomerization results in a difference of orders of magnitude in excited state lifetime.

It has been argued that a short excited state lifetime by virtue of rapid internal conversion is nature's strategy to protect the building blocks of life against UV induced damage that would otherwise result from slower photochemical processes. Figure 13 shows excited state lifetimes for the canonical bases in comparison with those for several of their derivatives. It appears that sub-picosecond lifetimes are a fairly unique property of the canonical bases and, as outlined above, this property is even specific to tautomers and base pair structures encountered in DNA. This would, however, not be a strategy that could have been adopted by biological evolution. For evolution to proceed, the replication machinery has to be in place first. Therefore any photochemical properties the bases have, must have originated from prebiotic times. Assuming that a primordial soup would have contained many possible variations of the heterocyclic compounds, it is conceivable that the building blocks of life underwent photochemical selection on an early earth. If so, these properties would be relics from chemistry that took place some four billion years ago.

In this context in needs to be remembered that gas phase spectroscopy constitutes a reductionist approach to the study of basic chemistry. Extrapolation to bulk conditions requires consideration of hydrogen bonding and stacking interactions. These interactions modify the photochemistry. For example, π stacking can lead to exciplex formation which opens up additional deexcitation channels (98).

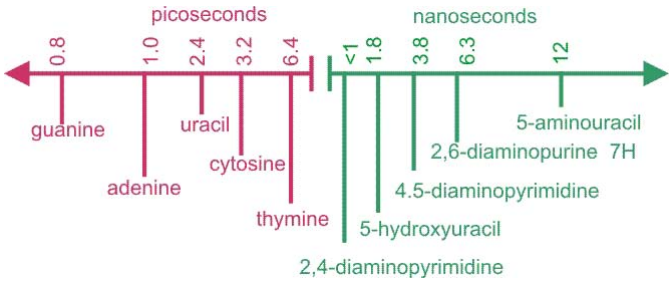

Figure 13: representative excited state lifetimes in the gas phase

6 Summary and outlook

The prime objective of gas phase studies is the investigation of intrinsic properties in *isolated* molecules. For a long time this approach has been limited to small molecules. The application to larger molecules is made possible by simultaneous progress in both experimental and computational technique. Laser desorption has made it possible to vaporize low vapour pressure neutral compounds intact and progress in computing power and theoretical treatments have made larger systems amenable to high level computation]. The resulting interplay between theory and experiment has been a powerful driver of this field of study. Theory has been instrumental in analysing and guiding experiments while at the same time gas-phase data are valuable for calibrating computational strategies. IR frequencies are among the best experimental data, available for this purpose. IR-UV DRS has emerged as a particularly fruitful meeting ground between theory and experiment, given its isomer selectivity. At this point even very high level computations still lack resolution, particularly in predicting hydrogen bond shifts and accounting for anharmonicity, so progress on this front may still be expected. It is still unclear what the molecular size limit is for this approach. The extrapolation from isolated molecules to bulk will likely be aided by studies of clusters. In addition to base pair clusters, work on several small clusters with water has been reported but data on larger clusters, at least approaching a first solvation shell, are still desirable.

A major use of IR data is structure determination, which for nucleobases includes tautomeric forms and cluster structures to model base pair interactions and microhydration. This capability also makes it possible to follow other properties as a function of structure. For the nucleobases it turns out that self-protection against UV photodamage by internal conversion depends dramatically on molecular structure. Comparison with solution experiments will likely further elucidate these findings and stimulate further research.

Acknowledgement

This material is based upon work supported by the National Science Foundation under CHE-1301305 and by NASA under Grant No. NNX12AG77G.

References

1. Kim, S.K., Lee, W. and Herschbach, D.H. (1996) Cluster Beam Chemistry: Hydration of Nucleic Acid Bases; Ionization Potentials of Hydrated Adenine and Thymine. *J. Phys. Chem.*, **100**, 7933-7937.
2. Anderson, J.B. and Fenn, J.B. (1965) Velocity Distributions in Molecular Beams from Nozzle Sources. *Physics of Fluids*, **8**, 780-&.
3. Levy, D.H. (1980) Laser Spectroscopy of Cold Gas-Phase Molecules. *Annu. Rev. Phys. Chem.*, **31**, 197-225.
4. Brady, B.B., Peteanu, L.A. and Levy, D.H. (1988) The Electronic Spectra of the Pyrimidine Bases Uracil and Thymine in a Supersonic Molecular Beam. *Chem. Phys. Lett.*, **147**, 538-543.
5. Plützer, C., Nir, E., de Vries, M.S. and Kleinermanns, K. (2001) IR-UV double-resonance spectroscopy of the nucleobase adenine. *PCCP*, **3**, 5466-5469.
6. Muller, A., Talbot, F. and Leutwyler, S. (2000) Intermolecular vibrations of jet-cooled (2-pyridone)/sub 2/: A model for the uracil dimer. *J. Chem. Phys.*, **112**, 3717-3725.
7. Muller, A., Talbot, F. and Leutwyler, S. (2001) Intermolecular vibrations of the jet-cooled 2-pyridone center dot 2-hydroxypyridine mixed dimer, a model for tautomeric nucleic acid base pairs. *J. Chem. Phys.*, **115**, 5192-5202.
8. Muller, A., Talbot, F. and Leutwyler, S. (2002) Hydrogen bond vibrations of 2-aminopyridine center dot 2-pyridone, a Watson-Crick analogue of adenine center dot uracil. *J. Am. Chem. Soc.*, **124**, 14486-14494.
9. Frey, J.A., Muller, A., Frey, H.M. and Leutwyler, S. (2004) Infrared depletion spectra of 2-aminopyridine center dot 2-pyridone, a Watson-Crick mimic of adenine center dot uracil. *J. Chem. Phys.*, **121**, 8237-8245.
10. Held, A. and Pratt, D.W. (1992) Hydrogen bonding in the symmetry-equivalent C/sub 2h/ dimer of 2-pyridone in its S/sub 0/ and S/sub 2/ electronic states. Effect of deuterium substitution. *J. Chem. Phys.*, **96**, 4869-4876.
11. Arrowsmith, P., de Vries, M.S., Hunziker, H.E. and Wendt, H.R. (1988) Pulsed laser desorption near a jet orifice: concentration profiles of entrained perylene vapor. *Appl. Phys. B*, **46**, 165-173.
12. Meijer, G., de Vries, M.S., Hunziker, H.E. and Wendt, H.R. (1990) Laser desorption jet-cooling of organic molecules. Cooling characteristics and detection sensitivity. *Appl. Phys. B*, **51**, 395-403.
13. Tembreull, R. and Lubman, D.M. (1987) Resonant Two-Photon Ionization of Small Peptides Using Pulsed Laser Desorption in Supersonic Beam Mass Spectrometry. *Anal. Chem.*, **59**, 1003-1006.
14. Weyssenhoff, H.V., Selzle, H.L. and Schlag, E.W. (1985) Laser-desorbed large molecules in a supersonic jet. *Zeitschrift fur Naturforschung, Teil A*, **40a**, 674-676.
15. Mayorkas, N., Malka, I. and Bar, I. (2011) Ionization-loss stimulated Raman spectroscopy for conformational probing of flexible molecules. *PCCP*, **13**, 6808-6815.

16. Lopez, J.C., Pena, M.I., Sanz, M.E. and Alonso, J.L. (2007) Probing thymine with laser ablation molecular beam Fourier transform microwave spectroscopy. *J. Chem. Phys.*, **126**.
17. Vaquero, V., Sanz, M.E., Lopez, J.C. and Alonso, J.L. (2007) The structure of uracil: A laser ablation rotational study. *J. Phys. Chem. A*, **111**, 3443-3445.
18. Alonso, J.L., Pena, I., Lopez, J.C. and Vaquero, V. (2009) Rotational Spectral Signatures of Four Tautomers of Guanine. *Angew Chem Int Edit*, **48**, 6141-6143.
19. Alonso, J.L., Vaquero, V., Pena, I., Lopez, J.C., Mata, S. and Caminati, W. (2013) All Five Forms of Cytosine Revealed in the Gas Phase. *Angew Chem Int Edit*, **52**, 2331-2334.
20. Lopez, J.C., Alonso, J.L., Pena, I. and Vaquero, V. (2010) Hydrogen bonding and structure of uracil-water and thymine-water complexes. *PCCP*, **12**, 14128-14134.
21. Merritt, J.M., Douberly, G.E. and Miller, R.E. (2004) Infrared-infrared-double resonance spectroscopy of cyanoacetylene in helium nanodroplets. *J. Chem. Phys.*, **121**, 1309-1316.
22. Choi, M.Y., Dong, F. and Miller, R.E. (2005) Multiple tautomers of cytosine identified and characterized by infrared laser spectroscopy in helium nanodroplets: probing structure using vibrational transition moment angles. *Philosophical Transactions of the Royal Society of London Series a-Mathematical Physical and Engineering Sciences*, **363**, 393-412.
23. Smolarek, S., Rijs, A.M., Buma, W.J. and Drabbels, M. (2010) Absorption spectroscopy of adenine, 9-methyladenine, and 2-aminopurine in helium nanodroplets. *PCCP*, **12**, 15600-15606.
24. Amirav, A., Even, U. and Jortner, J. (1981) Absorption-Spectroscopy of Ultracold Large Molecules in Planar Supersonic Expansions. *Chem. Phys. Lett.*, **83**, 1-4.
25. Liu, K., Fellers, R.S., Viant, M.R., McLaughlin, R.P., Brown, M.G. and Saykally, R.J. (1996) A long path length pulsed slit valve appropriate for high temperature operation: Infrared spectroscopy of jet-cooled large water clusters and nucleotide bases. *Rev. Sci. Instrum.*, **67**, 410-416.
26. Viant, M.R., Fellers, R.S., Mclaughlin, R.P. and Saykally, R.J. (1995) Infrared-Laser Spectroscopy of Uracil in a Pulsed Slit Jet. *J. Chem. Phys.*, **103**, 9502-9505.
27. Marian, C.M. (2007) The guanine tautomer puzzle: Quantum chemical investigation of ground and excited states. *J. Phys. Chem. A*, **111**, 1545-1553.
28. Mons, M., Dimicoli, I., Piuzzi, F., Tardivel, B. and Elhanine, M. (2002) Tautomerism of the DNA base guanine and its methylated derivatives as studied by gas-phase infrared and ultraviolet spectroscopy. *J. Phys. Chem. A*, **106**, 5088-5094.
29. Mons, M., Piuzzi, F., Dimicoli, I., Gorb, L. and Leszczynski, J. (2006) Near-UV resonant two-photon ionization spectroscopy of gas phase guanine: Evidence for the observation of three rare tautomers. *J. Phys. Chem. A*, **110**, 10921-10924.
30. Choi, M.Y. and Miller, R.E. (2006) Four tautomers of isolated guanine from infrared laser spectroscopy in helium nanodroplets. *J. Am. Chem. Soc.*, **128**, 7320-7328.

31. Nir, E., Janzen, C., Imhof, P., Kleinermanns, K. and de Vries, M.S. (2001) Guanine tautomerism revealed by UV-UV and IR-UV hole burning spectroscopy. *J. Chem. Phys.*, **115**, 4604-4611.
32. Seefeld, K., Brause, R., Häber, T. and Kleinermanns, K. (2007) Imino tautomers of gas-phase guanine from mid-infrared laser spectroscopy. *J. Phys. Chem. A*, **111**, 6217-6221.
33. Plützer, C. and Kleinermanns, K. (2002) Tautomers and electronic states of jet-cooled adenine investigated by double resonance spectroscopy. *PCCP*, **4**, 4877-4882.
34. Brown, R.D., Godfrey, P.D., McNaughton, D. and Pierlot, A. (1989) A Study of the Major Gas-phase Tatomer of Adenine by Microwave Spectroscopy. *Chem. Phys. Lett.*, **156**, 61-63.
35. Lee, Y., Schmitt, M., Kleinermanns, K. and Kim, B. (2006) Observation of ultraviolet rotational band contours of the DNA base adenine: Determination of the transition moment. *J. Phys. Chem. A*, **110**, 11819-11823.
36. Kim, N.J., Jeong, G., Kim, Y.S., Sung, J., Kim, S.K. and Park, Y.D. (2000) Resonant two-photon ionization and laser induced fluorescence spectroscopy of jet-cooled adenine. *J. Chem. Phys.*, **113**, 10051-10055.
37. Tomic, K., Tatchen, J. and Marian, C.M. (2005) Quantum chemical investigation of the electronic spectra of the keto, enol, and keto-imine tautomers of cytosine. *J. Phys. Chem. A*, **109**, 8410-8418.
38. Trygubenko, S.A., Bogdan, T.V., Rueda, M., Orozco, M., Luque, F.J., Sponer, J., Slavicek, P. and Hobza, P. (2002) Correlated ab initio study of nucleic acid bases and their tautomers in the gas phase, in a microhydrated environment and in aqueous solution - Part 1. Cytosine. *PCCP*, **4**, 4192-4203.
39. Kobayashi, R. (1998) A CCSD(T) study of the relative stabilities of cytosine tautomers. *J. Phys. Chem. A*, **102**, 10813-10817.
40. Szczesniak, M., Szczepaniak, K., Kwiatkowski, J.S., Kubulat, K. and Person, W.B. (1988) Matrix-isolation infrared studies of nucleic-acid constituents .5. Experimental matrix-isolation and theoretical abinitio scf molecular-orbital studies of the infrared-spectra of cytosine monomers. *J. Am. Chem. Soc.*, **110**, 8319-8330.
41. Brown, R.D., Godfrey, P.D., McNaughton, D. and Pierlot, A. (1989) Tautomers of Cytosine by Microwave Spectroscopy. *J. Am. Chem. Soc.*, **111**, 2308-2310.
42. Nir, E., Muller, M., Grace, L.I. and de Vries, M.S. (2002) REMPI spectroscopy of cytosine. *Chem. Phys. Lett.*, **355**, 59-64.
43. Nir, E., Hünig, I., Kleinermanns, K. and de Vries, M.S. (2003) The nucleobase cytosine and the cytosine dimer investigated by double resonance laser spectroscopy and ab initio calculations. *PCCP*, **5**, 4780-4785.
44. Nowak, M.J., Szczepaniak, K., Barski, A. and Shugar, D. (1978) Spectroscopic Studies on Vapor-Phase Tautomerism of Natural Bases Found in Nucleic-Acids. *Z Naturforsch C*, **33**, 876-883.
45. Brown, R.D., Godfrey, P.D., McNaughton, D. and Pierlot, A. (1988) The Microwave Spectrum of Uracil. *J. Am. Chem. Soc.*, **110**, 2329-2330.

46. Brown, R.D., Godfrey, P.D., Mcnaughton, D. and Pierlot, A.P. (1989) Microwave-Spectrum of the Major Gas-Phase Tautomer of Thymine. *J Chem Soc Chem Comm*, 37-38.
47. Kunitski, M., Nosenko, Y. and Brutschy, B. (2011) On the Nature of the Long-Lived "Dark" State of Isolated 1-Methylthymine. *ChemPhysChem*, **12**, 2024-2030.
48. van Zundert, G.C.P., Jaeqx, S., Berden, G., Bakker, J.M., Kleinermanns, K., Oomens, J. and Rijs, A.M. (2011) IR Spectroscopy of Isolated Neutral and Protonated Adenine and 9-Methyladenine. *ChemPhysChem*, **12**, 1921-1927.
49. Salpin, J.Y., Guillaumont, S., Tortajada, J., MacAleese, L., Lemaire, J. and Maitre, P. (2007) Infrared spectra of protonated uracil, thymine and cytosine. *ChemPhysChem*, **8**, 2235-2244.
50. Oomens, J., Moehlig, A.R. and Morton, T.H. (2010) Infrared Multiple Photon Dissociation (IRMPD) Spectroscopy of the Proton-Bound Dimer of 1-Methylcytosine in the Gas Phase. *J. Phys. Chem. Lett.*, **1**, 2891-2897.
51. Yang, B., Wu, R.R., Berden, G., Oomens, J. and Rodgers, M.T. (2013) Infrared Multiple Photon Dissociation Action Spectroscopy of Proton-Bound Dimers of Cytosine and Modified Cytosines: Effects of Modifications on Gas-Phase Conformations. *J. Phys. Chem. B*, **117**, 14191-14201.
52. Ung, H.U., Moehlig, A.R., Kudla, R.A., Mueller, L.J., Oomens, J., Berden, G. and Morton, T.H. (2013) Proton-bound dimers of 1-methylcytosine and its derivatives: vibrational and NMR spectroscopy. *PCCP*, **15**, 19001-19012.
53. Yang, B., Wu, R.R., Polfer, N.C., Berden, G., Oomens, J. and Rodgers, M.T. (2013) IRMPD Action Spectroscopy of Alkali Metal Cation-Cytosine Complexes: Effects of Alkali Metal Cation Size on Gas Phase Conformation. *J. Am. Soc. Mass. Spectrom.*, **24**, 1523-1533.
54. Nei, Y.W., Akinyemi, T.E., Kaczan, C.M., Steill, J.D., Berden, G., Oomens, J. and Rodgers, M.T. (2011) Infrared multiple photon dissociation action spectroscopy of sodiated uracil and thiouracils: Effects of thioketo-substitution on gas-phase conformation. *Int. J. Mass spectrom.*, **308**, 191-202.
55. Nei, Y.W., Akinyemi, T.E., Steill, J.D., Oomens, J. and Rodgers, M.T. (2010) Infrared multiple photon dissociation action spectroscopy of protonated uracil and thiouracils: Effects of thioketo-substitution on gas-phase conformation. *Int. J. Mass spectrom.*, **297**, 139-151.
56. Crampton, K.T., Rathur, A.I., Nei, Y.W., Berden, G., Oomens, J. and Rodgers, M.T. (2012) Protonation Preferentially Stabilizes Minor Tautomers of the Halouracils: IRMPD Action Spectroscopy and Theoretical Studies. *J. Am. Soc. Mass. Spectrom.*, **23**, 1469-1478.
57. Nei, Y.W., Crampton, K.T., Berden, G., Oomens, J. and Rodgers, M.T. (2013) Infrared Multiple Photon Dissociation Action Spectroscopy of Deprotonated RNA Mononucleotides: Gas-Phase Conformations and Energetics. *J. Phys. Chem. A*, **117**, 10634-10649.

58. Nei, Y.W., Hallowita, N., Steill, J.D., Oomens, J. and Rodgers, M.T. (2013) Infrared Multiple Photon Dissociation Action Spectroscopy of Deprotonated DNA Mononucleotides: Gas-Phase Conformations and Energetics. *J. Phys. Chem. A*, **117**, 1319-1335.
59. Ligare, M., Rijs, A.M., Berden, G., Kabelac, M., Nachtigallova, D., Oomens, J. and de Vries, M.S. (2014) Resonant IRMPD of Nucleotide Monophosphate Anionic Clusters. *Submitted*.
60. Nir, E., Janzen, C., Imhof, P., Kleinermanns, K. and de Vries, M.S. (2002) Pairing of the nucleobases guanine and cytosine in the gas phase studied by IR-UV double-resonance spectroscopy and ab initio calculations. *PCCP*, **4**, 732-739.
61. Mayorkas, N., Izbitski, S., Bernat, A. and Bar, I. (2012) Simultaneous Ionization-Detected Stimulated Raman and Visible-Visible-Ultraviolet Hole-Burning Spectra of Two Tryptamine Conformers. *J. Phys. Chem. Lett.*, **3**, 603-607.
62. Brauer, B., Gerber, R.B., Kabelac, M., Hobza, P., Bakker, J.M., Riziq, A.G.A. and de Vries, M.S. (2005) Vibrational spectroscopy of the G center dot center dot center dot C base pair: Experiment, harmonic and anharmonic calculations, and the nature of the anharmonic couplings. *J. Phys. Chem. A*, **109**, 6974-6984.
63. Plützer, C., Hünig, I., Kleinermanns, K., Nir, E. and de Vries, M.S. (2003) Pairing of isolated nucleobases: Double resonance laser spectroscopy of adenine-thymine. *ChemPhysChem*, **4**, 838-842.
64. Crews, B., Abo-Riziq, A., Grace, L., Callahan, M., Kabelac, M., Hobza, P. and de Vries, M.S. (2005) IR-UV double resonance spectroscopy of guanine-H2O clusters. *PCCP*, **7**, 3015-3020.
65. Chin, W., Mons, M., Piuzzi, F., Tardivel, B., Dimicoli, I., Gorb, L. and Leszczynski, J. (2004) Gas phase rotamers of the nucleobase 9-methylguanine enol and its monohydrate: Optical spectroscopy and quantum mechanical calculations. *J. Phys. Chem. A*, **108**, 8237-8243.
66. Piuzzi, F., Mons, M., Dimicoli, I., Tardivel, B. and Zhao, Q. (2001) Ultraviolet spectroscopy and tautomerism of the DNA base guanine and its hydrate formed in a supersonic jet. *Chem. Phys.*, **270**, 205-214.
67. Asami, H., Yagi, K., Ohba, M., Urashima, S. and Saigusa, H. (2013) Stacked base-pair structures of adenine nucleosides stabilized by the formation of hydrogen-bonding network involving the two sugar groups. *Chem. Phys.*, **419**, 84-89.
68. Saigusa, H., Urashima, S. and Asami, H. (2009) IR-UV Double Resonance Spectroscopy of the Hydrated Clusters of Guanosine and 9-Methylguanine: Evidence for Hydration Structures Involving the Sugar Group. *J. Phys. Chem. A*, **113**, 3455-3462.
69. Saigusa, H., Urashima, S., Asami, H. and Ohba, M. (2010) Microhydration of the Guanine-Guanine and Guanine-Cytosine Base Pairs. *J. Phys. Chem. A*, **114**, 11231-11237.
70. Zeleny, T., Hobza, P. and Kabelac, M. (2009) Microhydration of guanine center dot center dot center dot cytosine base pairs, a theoretical Study on the role of water in stability, structure and tautomeric equilibrium. *PCCP*, **11**, 3430-3435.

71. Kabelac, M., Ryjacek, F. and Hobza, P. (2000) Already two water molecules change planar H-bonded structures of the adenine ... thymine base pair to the stacked ones: a molecular dynamics simulations study. *PCCP*, **2**, 4906-4909.
72. Callahan, M.P., Gengeliczki, Z., Svadlenak, N., Valdes, H., Hobza, P. and de Vries, M.S. (2008) Non-standard base pairing and stacked structures in methyl xanthine clusters. *PCCP*, **10**, 2819-2826.
73. Callahan, M.P., Crews, B., Abo-Riziq, A., Grace, L., de Vries, M.S., Gengeliczki, Z., Holmes, T.M. and Hill, G.A. (2007) IR-UV double resonance spectroscopy of xanthine. *PCCP*, **9**, 4587-4591.
74. Plützer, C., Hünig, I. and Kleinermanns, K. (2003) Pairing of the nucleobase adenine studied by IR-UV double-resonance spectroscopy and ab initio calculations. *PCCP*, **5**, 1158-1163.
75. Smith, V.R., Samoylova, E., Ritze, H.H., Radloff, W. and Schultz, T. (2010) Excimer states in microhydrated adenine clusters. *PCCP*, **12**, 9632-9636.
76. Malone, R.J., Miller, A.M. and Kohler, B. (2003) Singlet Excited-state Lifetimes of Cytosine Derivatives Measured by Femtosecond Transient Absorption. *Photochem. Photobiol.*, **77**, 158-164.
77. Nachtigallova, D., Lischka, H., Szymczak, J.J., Barbatti, M., Hobza, P., Gengeliczki, Z., Pino, G., Callahan, M.P. and de Vries, M.S. (2010) The effect of C5 substitution on the photochemistry of uracil. *PCCP*, **12**, 4924-4933.
78. Mburu, E. and Matsika, S. (2008) An Ab Initio Study of Substituent Effects on the Excited States of Purine Derivatives. *J. Phys. Chem. A*, **112**, 12485-12491.
79. Kistler, K.A. and Matsika, S. (2007) Cytosine in context: A theoretical study of substituent effects on the excitation energies of 2-pyrimidinone derivatives. *J. Phys. Chem. A*, **111**, 8708-8716.
80. Broo, A. (1998) A theoretical investigation of the physical reason for the very different luminescence properties of the two isomers adenine and 2-aminopurine. *J. Phys. Chem. A*, **102**, 526-531.
81. Andreasson, J., Holmén, A. and Albinsson, B. (1999) The photophysical properties of the adenine chromophore. *J. Phys. Chem. B*, **103**, 9782-9789.
82. Kim, N.J., Jeong, G., Kim, Y.S., Sung, J., Kim, S.K. and Park, Y.D. (2000) Resonant two-photon ionization and laser induced fluorescence spectroscopy of jet-cooled adenine. *J. Chem. Phys.*, **113**, 10051-10055.
83. Mishra, S.K., Shukla, M.K. and Mishra, P.C. (2000) Electronic spectra of adenine and 2-aminopurine: an ab initio study of energy level diagrams of different tautomers in gas phase and aqueous solution. *Spectrochim. Acta, Part A*, **56**, 1355-1384.
84. Lührs, D.C., Viallon, J. and Fischer, I. (2001) Excited state spectroscopy and dynamics of isolated adenine and 9-methyladenine. *Phys. Chem. Chem. Phys.*, **3**, 1827-1831.
85. Kang, H., Jung, B. and Kim, S.K. (2003) Mechanism for ultrafast internal conversion of adenine. *J. Chem. Phys.*, **118**, 6717-6719.

86. Sobolewski, A.L. and Domcke, W. (2002) On the mechanism of nonradiative decay of DNA bases: ab initio and TDDFT results for the excited states of 9H-adenine. *Eur. Phys. J. D*, **20**, 369-374.
87. Barbatti, M. and Lischka, H. (2007) Can the Nonadiabatic Photodynamics of Aminopyrimidine Be a Model for the Ultrafast Deactivation of Adenine? *J. Phys. Chem. A*, **111**, 2852-2858.
88. Marian, C.M. (2005) A new pathway for the rapid decay of electronically excited adenine. *J. Chem. Phys.*, **122**, 104314.
89. Hünig, I., Plützer, C., Seefeld, K.A., Löwenich, D., Nispel, M. and Kleinermanns, K. (2004) Photostability of isolated and paired nucleobases: N-H dissociation of adenine and hydrogen transfer in its base pairs examined by laser spectroscopy. *ChemPhysChem*, **5**, 1427-1431.
90. Crespo-Hernández, C.E., Cohen, B., Hare, P.M. and Kohler, B. (2004) Ultrafast Excited-State Dynamics in Nucleic Acids. *Chem. Rev.*, **104**, 1977-2019.
91. Zierhut, M., Roth, W. and Fischer, I. (2004) Dynamics of H-atom loss in adenine. *PCCP*, **6**, 5178-5183.
92. Zechmann, G. and Barbatti, M. (2008) Ab initio study of the photochemistry of aminopyrimidine. *Int. J. Quantum Chem.*, **108**, 1266-1276.
93. Kistler, K.A. and Matsika, S. (2008) Three-state conical intersections in cytosine and pyrimidinone bases. *J. Chem. Phys.*, **128**, -.
94. Kistler, K.A. and Matsika, S. (2007) Radiationless decay mechanism of cytosine: An ab initio study with comparisons to the fluorescent analogue 5-methyl-2-pyrimidinone. *J. Phys. Chem. A*, **111**, 2650-2661.
95. Yarasi, S., Brost, P. and Loppnow, G.R. (2007) Initial excited-state structural dynamics of thymine are coincident with the expected photochemical dynamics. *J. Phys. Chem. A*, **111**, 5130-5135.
96. Sobolewski, A.L., Domcke, W. and Hättig, C. (2005) Tautomeric selectivity of the excited-state lifetime of guanine/cytosine base pairs: The role of electron-driven proton-transfer processes. *Proc. Natl. Acad. Sci. USA*, **102**, 17903-17906.
97. Abo-Riziq, A., Grace, L., Nir, E., Kabelac, M., Hobza, P. and de Vries, M.S. (2005) Photochemical selectivity in guanine-cytosine base-pair structures. *Proc. Natl. Acad. Sci. USA*, **102**, 20-23.
98. Middleton, C.T., de La Harpe, K., Su, C., Law, Y.K., Crespo-Hernandez, C.E. and Kohler, B. (2009) DNA Excited-State Dynamics: From Single Bases to the Double Helix. *Annu. Rev. Phys. Chem.*, **60**, 217-239.